THE JOURNAL OF BIOLOGICAL CHEMISTRY
Vol. 278, No. 44, Issue of October 31, pp. 43261–43267, 2003

Printed in U.S.A.

Modified Cardiovascular L-type Channels in Mice Lacking the Voltage-dependent Ca^{2+} Channel β3 Subunit*

Received for publication, November 7, 2002, and in revised form, August 12, 2003
Published, JBC Papers in Press, August 14, 2003, DOI 10.1074/jbc.M211380200

Manabu Murakami‡, Hisao Yamamura§, Takashi Suzuki¶, Myoung-Goo Kang‖, Susumu Ohya§, Agnieszka Murakami, Ichiro Miyoshi, Hironobu Sasano¶, Katsuhiko Muraki§, Takuzou Hano‡‡, Noriyuki Kasai**, Shinnsuke Nakayama§§, Kevin P. Campbell‖, Veit Flockerzi¶¶, Yuji Imaizumi§, Teruyuki Yanagisawa‖‖, and Toshihiko Iijima**

*From the Department of Pharmacology, Akita University School of Medicine, Akita 010-8543, the §Department of Molecular and Cellular Pharmacology, Graduate School of Pharmaceutical Sciences, Nagoya City University, Nagoya 467-8603, ¶Department of Pathology, **Institute for Animal Experimentation, and the ‖‖Department of Molecular Pharmacology, Tohoku University School of Medicine, Sendai 980-8575, ‡‡Division of Cardiology, the Department of Medicine, Wakayama Medical College, Wakayama 641-8509, the §§Department of Cell Physiology, Nagoya University Graduate School of Medicine, Tsuruma-cho, Shouwa, Nagoya 466-8550, Japan, the ‖Department of Physiology and Biophysics, Howard Hughes Medical Institute, University of Iowa, Iowa City, Iowa 52242 and ¶¶Institut für Pharmakologie und Toxikologie, Universität des Saarlandes, Hamburg 66421, Germany*

The β subunits of voltage-dependent calcium channels are known to modify calcium channel currents through pore-forming α_1 subunits. Of the four β subunits reported to date, the β3 subunit is highly expressed in smooth muscle cells and is thought to consist of L-type calcium channels. To determine the role of the β3 subunit in the voltage-dependent calcium channels of the cardiovascular system *in situ*, we performed a series of experiments in β3-null mice. Western blot analysis indicated a significant reduction in expression of the α_1 subunit in the plasma membrane of β3-null mice. Dihydropyridine binding experiments also revealed a significant decrease in the calcium channel population in the aorta. Electrophysiological analyses indicated a 30% reduction in Ca^{2+} channel current density, a slower inactivation rate, and a decreased dihydropyridine-sensitive current in β3-null mice. The reductions in the peak current density and inactivation rate were reproduced *in vitro* by co-expression of the calcium channel subunits in Chinese hamster ovary cells. Despite the reduced channel population, β3-null mice showed normal blood pressure, whereas a significant reduction in dihydropyridine responsiveness was observed. A high salt diet significantly elevated blood pressure only in the β3-null mice and resulted in hypertrophic changes in the aortic smooth muscle layer and cardiac enlargement. In conclusion, this study demonstrates the involvement and importance of the β3 subunit of voltage-dependent calcium channels in the cardiovascular system and in regulating channel populations and channel properties in vascular smooth muscle cells.

Voltage-dependent calcium channels (VDCCs)[1] are the main mediators of calcium entry in many cell types and play pivotal roles in the control of calcium-dependent cellular functions, such as smooth muscle contraction. These channels are classified electrophysiologically and pharmacologically into five groups (L, N, T, R, and P/Q). L-type calcium channels are crucial for excitation-contraction coupling as voltage sensors in skeletal muscle and as the main mediators of calcium entry in heart and smooth muscle tissues. VDCCs are composed of four subunits, α_1, α_2, δ, β, and γ (1, 2). The α_1 subunits are the pore-forming subunits and are targets of calcium channel blockers such as dihydropyridines (DHPs), phenylalkylamines, and benzothiazepines, which are widely used for the treatment of hypertension, angina pectoris, and cardiac arrhythmias. Ten genes encoding pore-forming α_1 subunits have been reported to date (3). The β subunits accelerate activation and inactivation of calcium channel currents, increase the channel population, and influence the coupling of gating charge movement; in addition, the $\beta\gamma$ dimer ($G\beta\gamma$) is thought to be involved in G protein-mediated channel inhibition (4–8). The β subunits are non-glycosylated hydrophilic proteins located on the intracellular side of the membrane; four variants are known (β1, β2, β3, and β4). Due to its wide expression in the aorta, trachea, and lung, β3 is considered the β subunit of smooth muscle calcium channels; it is also thought to couple with α_{1C} subunits and comprise L-type calcium channels in these cells (9, 10). Although the role of the β subunits has been investigated by heterologous co-expression studies and antisense experiments with cultured cells, little is known about the physiological importance of the β3 subunit *in situ*.

The purpose of the present study was to clarify the importance of the voltage-dependent calcium channel β3 subunit in the cardiovascular system by using gene-targeted mutant mice. We examined channel populations in the aorta, calcium channel currents in aortic smooth muscle cells, calcium sparks in response to high KCl, and expression patterns of calcium channel subunits in the cardiovascular system of β3-null mice. We also measured blood pressure and heart rate in β3-null mice and compared them with wild-type controls. β3-Null mice showed high blood pressure, hypertrophic changes in the aortic smooth muscle layer, and cardiac enlargement in response to a high salt diet.

EXPERIMENTAL PROCEDURES

The wild-type ($\beta3^{+/+}$) and β3-deficient ($\beta3^{-/-}$) mice were 12–16-week-old experimentally naive mice (11, 12). Animals were maintained

* This work was supported by grants-in-aid from the Ministry of Education, Culture, Sports, Science and Technology of Japan. The costs of publication of this article were defrayed in part by the payment of page charges. This article must therefore be hereby marked "*advertisement*" in accordance with 18 U.S.C. Section 1734 solely to indicate this fact.

‡ To whom correspondence should be addressed: Akita University School of Medicine, 1-1-1 Hondou, Akita 010-8543, Japan. Tel.: 81-18-834-8930; Fax: 81-18-834-8930; E-mail: manabumurakami@excite.co.jp.

[1] The abbreviations used are: VDCCs, Voltage-dependent calcium channels; DHP, dihydropyridine; RyR, ryanodine-sensitive calcium release; CHO, Chinese hamster ovary; RT, reverse transcriptase; GFP, green fluorescent protein.

at 22 ± 0.5 °C under a 12-h light-dark cycle. All experiments were conducted during the light phase of the cycle.

RNA Isolation and RT-PCR Analysis—Total RNA was isolated from the mouse aorta using an RNeasy extraction kit (Qiagen Inc., Valencia, CA). Reverse transcription reaction was performed in a solution of 10 pmol of oligo(dT) primer, 1 μg of RNA, 1× first strand cDNA buffer (Invitrogen), 10 mM dithiothreitol, 0.4 mM dNTPs, 40 units of RNAsin, and 200 units of Superscript II (Invitrogen), in a volume of 25 μl, at 42 °C for 45 min. β3 and β2 subunit-specific sequences were amplified by PCR with the following primers: MB3S (5′-CTC AAA CAG GAA CAG AAG GCC-3′) and MB3A (5′-CAT AGC CTT TCA GAG AGG GTC-3′), corresponding to the sequences of the murine β3 subunit ^{128}LKQEQKAR^{136} and ^{184}PSLKGYE^{191}; MB2S (5′-CTA GAG AAC ATG AGG CTA CAG-3′) and MB2A (5′-ACT GTT TGC ACT GGG CTT AGG-3′), corresponding to the sequences of the murine β2 subunit ^{130}LENMRLQ^{137} and ^{197}PKPSANS^{204}. RT-PCR amplification of the α_{1C} subunit was performed using the specific primers MA1C3 (5′-TTG GCC ATT GCG GTG GAC AAC CTG-3′) and MA1C4 (5′-CTG GAG TGC ATC CAT GTG TAT CTT G-3′), which generated a PCR product of 237 bp.

Western Blot Analysis—For analysis of α_1, β2a, and β3, the aorta was dissected from each mouse and homogenized in homogenization buffer containing 20 mM $Na_4O_7P_2$, 20 mM $NaH_2PO_4{\cdot}H_2O$, 1 mM $MgCl_2$, 0.3 mM sucrose, 0.5 mM EDTA, and a mixture of protease inhibitors. Aliquots of 100 μg of the homogenate from each mouse were resolved by 10% gradient SDS-PAGE and subjected to Western blot analysis as described previously (13). Polyclonal antibodies, rabbit 143 and sheep 49, specific for the calcium channel subunits β2a, β3, and α_{1C}, respectively, have been described previously (14).

Binding Assays—Partially purified aortic smooth muscle membranes were prepared and suspended in 50 mM Tris-HCl buffer (pH 7.4), as described previously (15). The membranes (0.2 mg/ml) were incubated in a final volume of 0.5 ml, in the dark, for 90 min at 25 °C, in the presence of (+)-[^{3}H]PN 200-110 (84 Ci/mmol; Amersham Biosciences). The free ligand concentration was varied between 0.05 and 1.2 nM. Nonspecific binding was defined using nicardipine (1.0 μM). Incubation was terminated by rapid filtration on Whatman GF/B filters and by washing the filters six times with 2 ml of ice-cold buffer. The retained radioactivity was determined by liquid scintillation counting.

Patch Clamp Recording—Whole-cell recordings were made as described previously (16). Isolated cells from the aorta were voltage-clamped in whole-cell mode using a patch clamp amplifier EPC-7 (List, Lambrecht, Germany). The pipettes (3–5 megohms) were filled with a solution containing 140 mM CsCl, 4.0 mM $MgCl_2$, 5.0 mM EGTA, 5.0 mM Na_2ATP, and 10 mM HEPES. The pH was adjusted to 7.2 with 1 N CsOH. The bath solution contained 92 mM NaCl, 5.9 mM KCl, 30 mM $BaCl_2$, 1.2 mM $MgCl_2$, 14 mM glucose, and 10 mM HEPES. The pH was adjusted to 7.4 with 10 N NaOH. Whole-cell currents were elicited by 150-ms voltage clamp steps, from −50 to +60 mV, every 15 s, from the holding potential of −60 mV. Whole-cell currents were displayed without any leak subtraction, and membrane potentials have been corrected for junction potentials according to the method of Neher (17). Cell capacitance was measured by dividing the charge (Q) during the capacitative surge elicited by 10 mV hyperpolarization (ΔV) from −60 mV, using the equation $Cm = Q/\Delta V$. Data acquisition and analysis were done on a computer using software (Cell Soft) developed at the University of Calgary, Canada. Pooled data are shown as the mean ± S.E. The statistical significance of differences between $\beta3^{+/+}$ and $\beta3^{-/-}$ mice was determined using Student's unpaired t test.

Calcium Spark Measurement—The first branch mesenteric arteries (300–500 μm in diameter, 5 mm in length) were removed and placed into ice-cold, oxygenated (95% O_2, 5% CO_2) Krebs solution containing 112 mM NaCl, 4.7 mM KCl, 25 mM $NaHCO_3$, 1.2 mM KH_2PO_4, 2.2 mM $CaCl_2$, 1.2 mM $MgCl_2$, 0.023 mM EDTA, and 14 mM glucose (pH 7.4). The endothelium of the artery was gently wiped off. The arterial segment was incubated with Krebs solution containing 10 μM fluo-3-AM (Molecular Probes, Eugene, OR), 0.09% pluronic F-127, and 1 μM wortmannin, a myosin light chain kinase inhibitor, to suppress the movement of smooth muscle cells at room temperature (24 ± 1 °C) for 60 min. After incubation, the arterial strip was placed in the recording chamber using a stainless steel ring and was continuously perfused with standard HEPES-buffered solution at a flow rate of 5 ml/min. Standard HEPES-buffered solution has an ionic composition of 137 mM NaCl, 5.9 mM KCl, 2.2 mM $CaCl_2$, 1.2 mM $MgCl_2$, 14 mM glucose, and 10 mM HEPES. The pH of the solutions was adjusted to 7.4 with NaOH. Arteries were imaged using a fast scanning confocal microscope (Nikon RCM-8000; Nikon, Tokyo, Japan) equipped with an objective lens (Fluor 40 × 1.15 NA, water immersion, Nikon). The excitation wavelength from an argon ion laser was 488 nm, and the emission wavelength was 515 nm. The resolution of the microscope was ~0.33 × 0.27 (1 pixel) and ~2.2 μm in the z axis direction. The Ca^{2+} image required 33 ms to scan a full frame (512 × 512 pixels) and took 3.3 s to obtain 100 images in each trial at room temperature. Depolarization stimuli were applied by perfusion with HEPES-buffered solution containing 30 mM KCl. Pooled data are shown as the means ± S.E. The statistical significance of differences between groups was determined using Scheffé's test after one-way analysis of variance.

Measurement of Blood Pressure—Mice were age-matched between the groups and were trained several times before measurements. The heart rate and systolic and diastolic blood pressure were measured using an automated computerized system with the tail-cuff method (BP-98A; Softron, Tokyo, Japan). The animals were fed the high salt diet for 2 weeks before the experiments. Multivariate differences were analyzed by repeated measured analysis of variance. Results are given as means ± S.E.

Tissue Preparation and Histology—Tissues of $\beta3^{+/+}$ and $\beta3^{-/-}$ mice were excised under ether anesthesia. The tissues were fixed immediately in 4% paraformaldehyde in 0.1 M sodium phosphate buffer (pH 7.2) overnight at 4 °C and embedded in paraffin wax. Histological examination of slides stained with hematoxylin-eosin was performed.

Immunohistology—Immunohistochemical analysis was performed using the streptavidin-biotin amplification method. After deparaffinization, slides were treated with Pronase. The antigen-antibody complex was visualized as a brown precipitate with 3.3′-diaminobenzidine solution (1 mM diaminobenzidine, 50 mM Tris-HCl buffer (pH 7.6), and 0.006% H_2O_2), and counterstaining was performed with hematoxylin. Normal goat serum (1%) was applied to the sections for 20 min at room temperature, followed by the primary antibody at a dilution of 1:200 for 18 h at 4 °C. Commercially available antibodies that specifically recognize the α_{1C} subunit (Alomone, Jerusalem, Israel) were used. Sections were reacted with Envision plus (Dako, Copenhagen, Denmark) to visualize the antigen-antibody complex.

Whole-cell immunofluorescence labeling of isolated smooth muscle cells was tested with anti-β3 antibody at a dilution of 1:100 (Alomone) as the primary antibody, and further analyzed with fluorescein-conjugated polyclonal goat anti-rabbit IgG at a dilution of 1:200.

Electrophysiology with CHO Cells—Chinese hamster ovary (CHO) cells were cultured in Dulbecco's modified Eagle's medium, supplemented with 10% dialyzed fetal bovine serum. For electrical recordings, CHO cells at 30–50% confluence were plated onto 22-mm coverslips. Some CHO cells were transfected with an expression vector carrying the cloned smooth muscle α_{1C} subunit ($Ca_v1.2b$) in pcDNA3.1(+) (Invitrogen) and/or the β2a in pTracer (Invitrogen) and/or the β3 subunit in pcDNA3 (Invitrogen) with or without a green fluorescent protein (GFP) expression vector (pTracer) by lipofection (Superfect Transfection Reagent; Qiagen, Tokyo, Japan) (18). Expression of the channel subunits was quantified by the emission of green light using an IX70 fluorescence microscope (Olympus, Tokyo, Japan). Whole-cell patch clamp recording was carried out 48–72 h after transfection. Whole-cell currents were elicited by 3000-ms voltage clamp steps, from the holding potential at −60 to +10 mV every 15 s.

Statistics—The data are expressed as the means ± S.E. Differences were evaluated using unpaired t tests, unless stated otherwise. The level of statistical significance was $p < 0.05$.

RESULTS

β3 and β2 are Expressed in the Murine Aorta—RNA products derived from $\beta3^{+/+}$ and $\beta3^{-/-}$ mice were analyzed using the β3-specific primers, MB3S and MB3A, and β2-specific primers, MB2S and MB2A. RT-PCR analysis of the wild-type aorta showed β3- and β2-specific bands of 187 and 222 bp, respectively (Fig. 1*A*), indicating the expression of both subunits in this tissue. We also performed the experiment with β1- and β4-specific primers, which yielded no PCR products (data not shown). The expression of the α_{1C} subunit gene was confirmed in both wild-type and mutant mice. We also confirmed the expression of β2, β3, and α_{1C} subunit genes with other primer sets. Moreover, we also performed the experiment with primers for other α_1 subunits thought to participate in the formation of high voltage-activated calcium channels, such as α_{1A}, but PCR yielded no products with these primers.

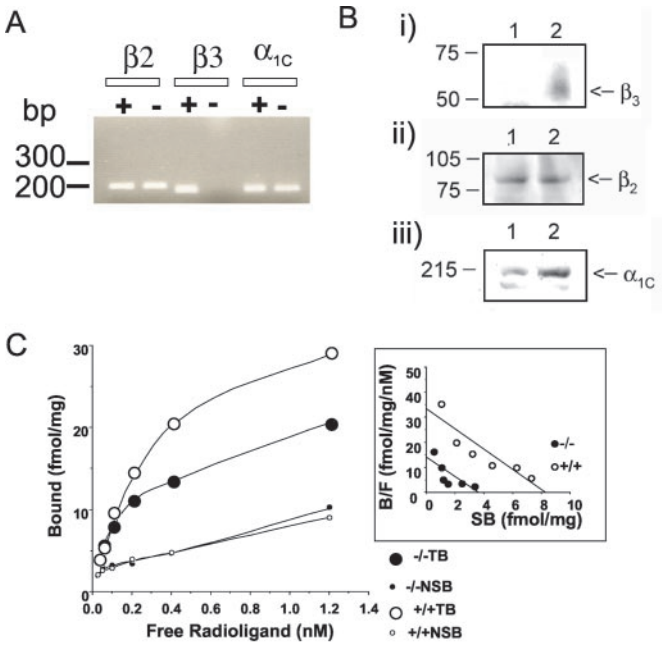

FIG. 1. *A*, identification of β2, β3, and α_{1C}-specific transcripts in the murine aorta (+, wild-type; −, β3-deficient). Primer sets used for each PCR amplification are indicated *above the open boxes. B*, Western blot analysis of the aortic plasma membranes. Membrane proteins (100 μg/lane) were probed with the following rabbit polyclonal antibodies. *i,* anti-β3 antibody: *lane 1*, $\beta3^{-/-}$; *lane 2*, $\beta3^{+/+}$. *ii,* anti-β2 antibody: *lane 1*, $\beta3^{-/-}$; *lane 2*, $\beta3^{+/+}$. *iii,* anti-α_{1C} antibody: *lane 1*, $\beta3^{-/-}$; *lane 2*, $\beta3^{+/+}$. *C*, Representative binding curves for (+)-[^{3}H]PN 200-110 in aortic smooth muscle. Total binding (*TB*, *large circles*) and nonspecific binding (*NSB*, *small circles*) in $\beta3^{+/+}$ (*open circles*) and $\beta3^{-/-}$ (*closed circles*) mice. *Inset,* Scatchard transformation of equilibrium binding of $\beta3^{+/+}$ (*open circles*) and $\beta3^{-/-}$ (*closed circles*) mice.

Reduced Calcium Channel Population by Disruption of the β3 Subunit

Western Blot Analysis—To confirm the deficiency of the β3 subunit and the expression of the β2 subunit in the aortic tissue at the protein level, we performed Western blot analysis using anti-β2, anti-β3, and anti-α_{1C} subunit antibodies. A single band corresponding to β3 was detected in $\beta3^{+/+}$ mice, whereas no corresponding band was detected in $\beta3^{-/-}$ mice (Fig. 1*B*). Anti-β2 antibody detected a single band of 84 kDa in $\beta3^{+/+}$ mice, indicating β2 subunit expression and suggesting that this subunit is a component of voltage-dependent calcium channels in the vascular tissue. There was no significant difference in the level of β2 subunit expression in the aortas of $\beta3^{-/-}$ mice, as compared with $\beta3^{+/+}$ controls, suggesting that there was no compensatory increase in the level of β2 expression in this tissue. On Western blot analysis, a single band with a molecular mass of 210 kDa was detected in the aortas of $\beta3^{+/+}$ and $\beta3^{-/-}$ mice with the anti-α_{1C} subunit antibody. We also performed Western blot analysis with anti-pan α_1 antibody, with the same results, suggesting that the majority of calcium channels are encoded by a single α_{1C} subunit gene that forms VDCCs in the mammalian cardiovascular system. $\beta3^{-/-}$ mice showed a reduced amount of the α_{1C} subunit in the aortic plasma membrane (~45% reduction as determined by densitometry), which suggested a decrease in the channel population in the smooth muscle cell membrane by the targeted disruption of the β3 subunit gene.

Binding Studies—To characterize further the decrease in the channel population, we next performed saturation binding analyses using the dihydropyridine derivative (+)-[^{3}H]PN 200-110, which binds to a saturable, non-interacting set of binding sites in aortic smooth muscle membranes. Fig. 1*C* shows typical results from a saturation experiment. The K_d values were 0.248 ± 0.072 nM ($\beta3^{+/+}$, $n = 4$) and 0.257 ± 0.064 nM ($\beta3^{-/-}$, $n = 4$), and the B_{max} values were 8.27 ± 0.51 fmol/mg protein ($\beta3^{+/+}$) and 3.68 ± 0.42 fmol/mg protein ($\beta3^{-/-}$) (Fig. 1*C, inset*), suggesting a decrease in the number of DHP receptors in the cell membrane (~56% reduction) of the mutant mice, with no apparent changes in the channel affinity. This 56% reduction in the channel population coincided with a similar reduction in the level of expression of α_1 subunits detected by Western blot analysis. The nonspecific binding values were quite high (about 30%), which made subsequent Scatchard analysis difficult in comparison to skeletal muscle membrane preparations, whose nonspecific binding value was about 10% (K_d = 0.287 nM, B_{max} = 401.15 fmol/mg protein).

Reduction and Modulation of Voltage-dependent Calcium Channel Currents—Whole-cell patch clamping was used to examine the effect of β3 expression on voltage-dependent Ca^{2+} channel currents in freshly dissociated aortic smooth muscle cells. The mean cell capacitance was 26.9 ± 1.1 in $\beta3^{+/+}$ cells and 24.4 ± 1.0 pF in $\beta3^{-/-}$ cells (13 cells from 7 mice for each, $p > 0.05$), respectively. Rectangular pulses (150-ms duration) of various potentials were applied in the presence of 30 mM Ba^{2+}, as a charge carrier. Fig. 2*A* shows examples of voltage-dependent Ca^{2+} channel currents. At positive test potentials, inward Ba^{2+} currents were observed in both $\beta3^{+/+}$ and $\beta3^{-/-}$ cells (Fig. 2*A*). In Fig. 2*B*, the density of the peak inward current was plotted against the test potential (I-V relationship). The density of the voltage-dependent inward current was, however, maximal at +10 mV irrespective of β3 expression. A reduction of about 30% in the Ca^{2+}-channel current density was observed in $\beta3^{-/-}$ cells (0.84 ± 0.08 pA/pF, $n = 12$ *versus* $\beta3^{+/+}$, 1.22 ± 0.10 pA/pF, $n = 7$, $p < 0.05$), in which the peak current was observed at +10 mV (Fig. 2*B*). Next, DHP sensitivity was examined with nicardipine. In both groups, the inward currents were effectively inhibited by 100 nM nicardipine, but a significant decrease was observed in the DHP-sensitive component in $\beta3^{-/-}$ cells (0.61 ± 0.10 pA/pF, $n = 7$, $p < 0.05$ *versus* $\beta3^{+/+}$, 0.99 ± 0.13 pA/pF, $n = 7$, Fig. 2*C*).

By contrast, inactivation of the voltage-dependent Ca^{2+} channel current was significantly slower in $\beta3^{-/-}$ cells. The decay time constant of the voltage-dependent Ca^{2+} channel current evoked at +10 mV was well fitted by an exponential function; the time constant was 59.2 ± 6.2 and 109.1 ± 7.4 ms in $\beta3^{+/+}$ cells ($n = 7$) and $\beta3^{-/-}$ cells ($n = 12$), respectively ($p < 0.01$, Fig. 2*D*). This is consistent with the observation that the inactivation was altered by different β subunits (9).

Decreased Responsiveness to Diltiazem in Global $[Ca^{2+}]_i$ and No Changes in Ca^{2+} Sparks—It has been suggested that VDCCs play an important role in coupling sparks and spontaneous transient outward currents, and that this coupling represents a negative feedback mechanism for regulating arterial tone. Therefore, Ca^{2+} sparks in intact mesenteric arteries were further examined.

Fig. 3*A* shows typical recordings of Ca^{2+} changes in the first branch of a wild-type mesenteric artery, in response to 30 mM KCl. This elevation of external K^+ increased global $[Ca^{2+}]_i$ in both $\beta3^{+/+}$ and $\beta3^{-/-}$ mice (F/F_0 increases of 1.34- and 1.21-fold in $\beta3^{+/+}$ and $\beta3^{-/-}$, respectively; Fig. 3*B*). The decrease in the global $[Ca^{2+}]_i$ in $\beta3^{+/+}$ mice on application of an L-type calcium channel blocker, diltiazem, was significantly larger than that in $\beta3^{-/-}$ mice (Fig. 3, *B* and *C*), suggesting decreased responsiveness to diltiazem in the mutants. However, there were no significant differences in the amplitudes of local $[Ca^{2+}]_i$ transients (Ca^{2+} sparks, >100 ms in half-duration) between $\beta3^{+/+}$ ($n = 18$) and $\beta3^{-/-}$ cells ($n = 24$) from 5 mice each in either standard or high KCl solutions or in the presence

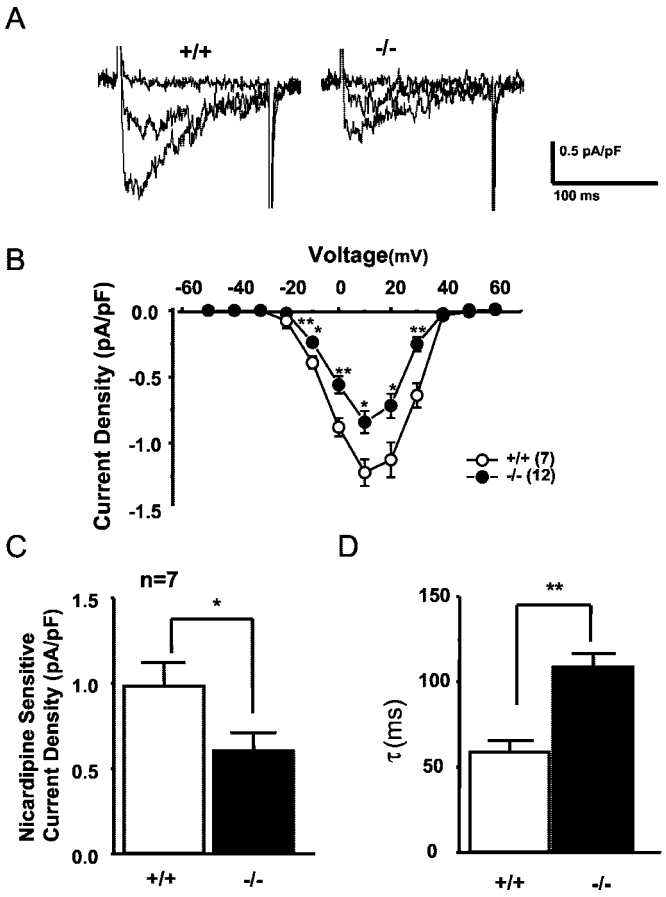

FIG. 2. **Calcium channel currents recorded in the aortic smooth muscle cells.** *A*, representative traces of voltage-dependent Ca^{2+} channel currents in murine aortic smooth muscle from $\beta3^{+/+}$ (+/+) and $\beta3^{-/-}$ (−/−) mice. Cells were depolarized from the holding potential of −60 to −30, −10, and +10 mV for 150 ms. *B*, I-V curves generated by 150-ms depolarization pulses from a holding potential of −60 mV to potentials between −50 and +60 mV in $\beta3^{+/+}$ ($n = 7$, *open circles*) and $\beta3^{-/-}$ ($n = 12$, *closed circles*) cells. The current density was estimated by dividing the peak amplitude by the cell capacitance (pA/pF). *C*, effects of nicardipine on I_{Ba} current in $\beta3^{+/+}$ ($n = 7$, *open bar*) and $\beta3^{-/-}$ ($n = 7$, *closed bar*) cells. Cells were depolarized every 15 s from the holding potential of −60 to 0 mV for 150 ms. After stabilization of I_{Ba}, 100 nM nicardipine was applied. *D*, the time constants of the I_{Ba} decay in $\beta3^{+/+}$ ($n = 7$, *open bar*) and $\beta3^{-/-}$ ($n = 12$, *closed bar*) cells. The numbers of myocytes used are given in *parentheses*. The statistical significance of the difference between $\beta3^{+/+}$ and $\beta3^{-/-}$ mice is indicated by *, $p < 0.05$, or **, $p < 0.01$.

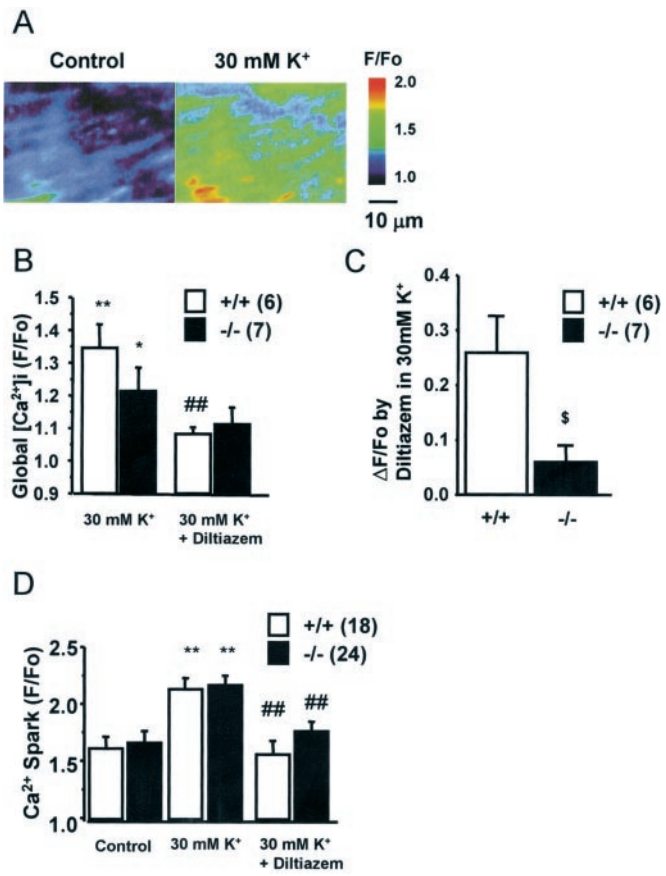

FIG. 3. *A*, typical recordings of Ca^{2+} changes in response to a depolarizing solution of 30 mM KCl in the first branch of the mesenteric artery in $\beta3^{+/+}$ mice. The $[Ca^{2+}]_i$ (F/F_0) is expressed using pseudocolors. *B*, changes in global $[Ca^{2+}]_i$ in response to KCl, and the inhibitory effect of diltiazem in $\beta3^{+/+}$ ($n = 6$, *open bars*) and $\beta3^{-/-}$ ($n = 7$, *closed bars*) mice. *C*, the diltiazem-sensitive changes in global $[Ca^{2+}]_i$ with 30 mM K^+ in $\beta3^{+/+}$ ($n = 6$, *open bar*) and $\beta3^{-/-}$ ($n = 7$, *closed bar*) mice are shown based on the results in *B*. *D*, changes in the fluorescence intensity in the Ca^{2+} sparks in response to 30 mM KCl, and the inhibitory effect of diltiazem in $\beta3^{+/+}$ ($n = 18$, *open bars*) and $\beta3^{-/-}$ ($n = 24$, *closed bars*) mice. The number of myocytes used is given in *parentheses*. The statistical significance of the difference between control and 30 mM K^+ is indicated by *, $p < 0.05$, and **, $p < 0.01$. The difference between 30 mM K^+ and 30 mM K^+ + diltiazem is shown by ##, $p < 0.01$. The difference between $\beta3^{+/+}$ and $\beta3^{-/-}$ mice is shown by \$, $p < 0.05$.

of diltiazem (Fig. 3*D*). The frequency of Ca^{2+} sparks was also not affected significantly by β3 deficiency (0.22 ± 0.05 and 0.18 ± 0.04 Hz in $\beta3^{+/+}$ and $\beta3^{-/-}$ cells, respectively, in standard solution, $p > 0.05$). The characteristics of longer periodical Ca^{2+} events (Ca^{2+} waves) were also detected in these preparations. The amplitude (F/F_0) and frequency were 1.79 ± 0.03 and 0.13 ± 0.05 Hz, respectively, in $\beta3^{+/+}$ cells (13 cells from 5 mice) and were not significantly different from those in $\beta3^{-/-}$ cells (1.98 ± 0.16 and 0.15 ± 0.04 Hz, respectively, 14 cells from 5 mice).

β3 Subunit Expression Pattern

Immunohistological Examination of the α_{1C} Subunit in the Heart and Aorta—To evaluate the decrease in channel population identified by Western blot and DHP binding analyses, we examined the distribution of the α_{1C} subunit, of which the majority of L-type channels in the heart and aorta is comprised. The α_{1C} subunit is distributed homogeneously in the heart and aortic smooth muscle cell layer. There were no clear differences in the patterns of immunohistological labeling between wild-type and mutant mice (Fig. 4*A*). Conventional immunohistological labeling with streptavidin-biotin amplification did not allow us to detect the distribution of the β3 subunit, as the levels of background signals were high. Therefore, we examined expression of the β3 subunit by whole-cell fluorescence immunohistochemical analysis in isolated aortic smooth muscle cells (Fig. 4*B, left panels*). In the wild-type mice (Fig. 4*Bi*), a homogeneous distribution of the β3 subunit was observed, whereas only background signals were detected in $\beta3^{-/-}$ mice (Fig. 4*Bii*, *inset* has high signal intensification, resulting in high background signals). The corresponding phase contrast images are shown in the *right panels*.

Decreased Responsiveness to Amlodipine and Salt-sensitive Increase in Blood Pressure—The significance of the L-type voltage-dependent calcium channels in the cardiovascular system is widely known, and its blockers, such as DHP, are widely used in the treatment of hypertension. Therefore, decreased blood pressure was anticipated, but no significant differences were observed in systolic or diastolic blood pressure in $\beta3^{-/-}$ mice on normal diets, as compared with wild-type controls. We also measured blood pressure using arterial catheters. As there were no significant differences in the results obtained using the

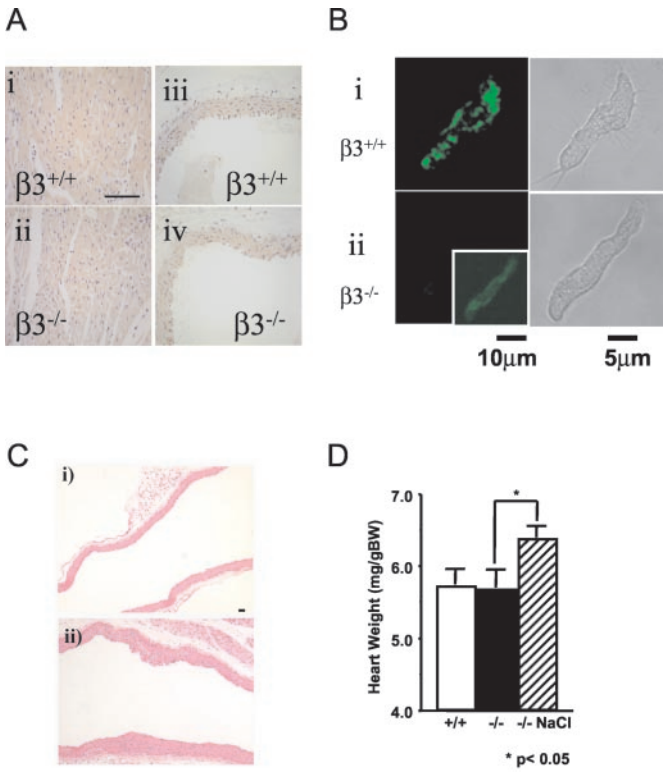

FIG. 4. *A*, immunohistological localization of α_{1C} subunits in the heart (*i* and *ii*, wild-type and mutant mice, respectively) and in the aorta (*iii* and *iv*, wild-type and mutant mice, respectively). *Scale bar* = 50 μm. *B*, whole-cell fluorescence immunohistochemistry of the β3 subunit in isolated aortic smooth muscle cells (*left panels*, *i* and *ii*, $\beta3^{+/+}$ and $\beta3^{-/-}$ cells, respectively) and corresponding phase-contrast images (*right panels*). *Scale bar* = 5 and 10 μm (*inset*). The *inset* is an intensified signal of a $\beta3^{-/-}$ cell. *C*, hematoxylin-eosin staining of the aorta of $\beta3^{-/-}$ mice without (*i*) or with (*ii*) high salt diet. *Scale bar* = 50 μm. *D*, heart weight of $\beta3^{+/+}$ (*open bar*, $n = 9$) and $\beta3^{-/-}$ mice, without (*closed bar*, $n = 10$) and with (*hatched bar*, $n = 11$) the high salt diet. Data are expressed as means ± S.E. *, $p < 0.05$.

tail-cuff and intra-arterial methods, we used the tail-cuff method for subsequent measurements.

Intraperitoneal injection of amlodipine (1.0 mg/kg), a DHP analogue significantly lowered systolic and diastolic blood pressure in $\beta3^{+/+}$ mice, whereas it had no significant effect in $\beta3^{-/-}$ mice (Table I).

As high dietary salt intake in humans is associated with high blood pressure (19), we next examined the effects of a high salt diet, containing 8% NaCl, on the blood pressure of $\beta3^{+/+}$ and $\beta3^{-/-}$ mice. Loading with the high salt diet for 2 weeks increased systolic and diastolic blood pressure in $\beta3^{-/-}$ mice but not in $\beta3^{+/+}$ mice (Table I). Loading with the high salt diet for 3 months induced hypertrophic changes in the aortic smooth muscle of $\beta3^{-/-}$ mice (Fig. 4*C*), whereas no significant changes were observed in $\beta3^{+/+}$ mice. Mutant $\beta3^{-/-}$ mice on the high salt diet also showed an increase in heart weight (Fig. 4*D*). As these pathological changes are common features in hypertensive animals, they may have been a consequence of elevated blood pressure.

Electrophysiological Recordings of Transiently Transfected Cav1.2b-expressing CHO Cells—To analyze further the importance of β subunits in the voltage-dependent calcium channels in smooth muscle cells, we next analyzed transient expression of the Cav1.2b, β2, and β3 subunits in CHO cells. Fig. 5*A* shows representative whole-cell Ca^{2+} channel currents recorded using Ba^{2+} as the charge carrier. A rectangular 10-mV pulse (3000 ms in duration) was applied. The mean cell capacitance was 16.0 ± 0.4 pF.

TABLE I

+/+, $\beta3^{+/+}$ without treatment; −/−, $\beta3^{-/-}$ without treatment; +/+ amlodipine (amlo), $\beta3^{+/+}$ 60 min after injection of amlodipine (1.0 mg/kg); −/−, $\beta3^{-/-}$ 60 min after injection of amlodipine (1.0 mg/kg); +/+ NaCl, $\beta3^{+/+}$ after 2 weeks of NaCl loading; −/− NaCl, $\beta3^{-/-}$ after 2 weeks of NaCl loading. Effects of disruption of the β3 subunit on systolic (SBP) and diastolic (DBP) blood pressure in mice on normal and high salt diets. Each value represents the mean ± S.E. Each group consisted of 35 mice from 9 to 12 weeks old.

	Heart rate	SBP	DBP
	beats/min	*mm Hg*	
+/+	628 ± 8	98.5 ± 1.9	60.9 ± 1.6
−/−	619 ± 14	97.0 ± 1.9	60.4 ± 1.6
+/+ amlo	686 ± 9[a]	87.2 ± 2.0[a]	51.3 ± 2.4[a]
−/− amlo	622 ± 19	98.2 ± 2.1	57.8 ± 2.7
+/+ NaCl	631 ± 13	97.9 ± 1.8	65.4 ± 1.1
−/− NaCl	627 ± 11	113.1 ± 1.9[b]	71.7 ± 1.4[b]

[a] $p < 0.01$ *versus* +/+.
[b] $p < 0.01$ *versus* −/−.

To examine whether transfection itself influences the Ca^{2+} channel current, we first transfected CHO cells with a GFP plasmid alone (pTracer). This mock transfection had no effect on voltage-dependent Ca^{2+} channel currents (Fig. 5*Ai*). The voltage-dependent inward Ca^{2+} channel current (Fig. 5*Aii*) was recorded from CHO cells transiently expressing α_{1C} (Cav1.2b) with GFP plasmid (α_{1C}/Mock). In the CHO cells expressing α_{1C}, the current density estimated from the peak inward current at 10 mV (PCD_{10mV}) was 10.7 ± 0.5 pA/pF ($n = 8$). The voltage-dependent inward current decayed very slowly during depolarization (time constant, 868.0 ± 11.8 ms, $n = 8$). These features are essentially the same as reported previously (20, 21).

The inward Ba^{2+} currents (Fig. 5*A, iii–v*) were recorded from CHO cells in which the β2a subunit alone (*iii*), the β2a and β3 subunits simultaneously (*iv*), or β3 alone (*v*) were transiently expressed with α_{1C}. Fig. 5*B* summarizes the effects of expressing β subunits on PCD_{10mV}. Expression of either β subunit significantly increased PCD_{10mV} (*iii*, 20.0 ± 1.0 pA/pF, $n = 8$; *iv*, 21.6 ± 0.8 pA/pF, $n = 8$; *v*, 23.0 ± 1.0 pA/pF, $n = 8$). There were, however, no statistically significant differences ($p > 0.05$) between the three groups.

Expression of the β3 subunit significantly accelerated the rate of inactivation. The time constant (τ) for each combination is summarized in Fig. 5*C*. CHO cells, expressing α_{1C} with GFP plasmid (α_{1C}/Mock), were inactivated very slowly. Of the three types of β-expressing CHO cells, the decay was fastest with β3 alone (time constant, 528.4 ± 18.2 ms, $n = 8$) and slowest with β2 alone (time constant, 975.1 ± 31.0 ms, $n = 8$). The latter is thought to mimic $\beta3^{-/-}$ aortic smooth muscle cells. The rate of inactivation for the transient expression of β2 alone significantly differed from the inactivation rates for the other two cases. The combined expression of the β2 and β3 subunits had an intermediate effect (time constant, 669.1 ± 19.9 ms, $n = 8$). Overall, β3 had qualitatively the same effects in this expression system (CHO cells) as in the isolated smooth muscle cells of β3-deficient mice.

In addition, to address whether transfection of β subunits invokes expression of some endogenous voltage-dependent Ca^{2+} channels, we transfected the β3 subunit in CHO cells. Even after expressing the β3 subunit, step depolarization did not evoke an inward Ca^{2+} channel current (data not shown). Essentially the same results were obtained on transfecting β2 instead of β3 (data not shown).

The results of these electrophysiological experiments indicated that there were differences between the channel properties in cells co-expressing α_{1C}, β2a, and β3 subunits. Furthermore, the β3 subunit markedly accelerated current decay as compared with the β2 subunit, suggesting that the significant

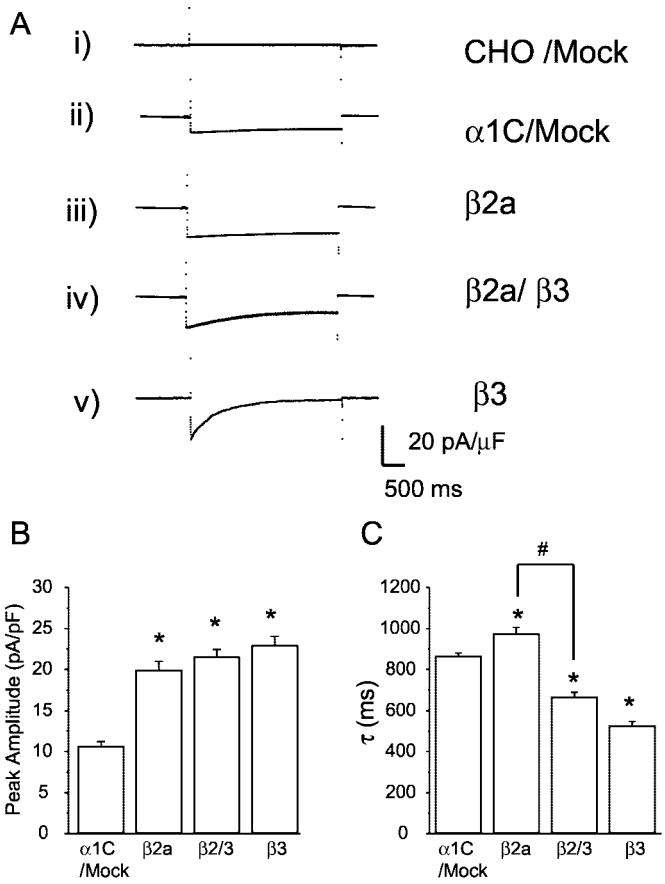

FIG. 5. *A*, representative current traces obtained from CHO cells expressing GFP alone (*CHO/Mock*) (*i*), α_{1C} with GFP (α_{1C}/*Mock*) (*ii*), and *β2a* (*iii*), *β2a/β3* (*iv*), and *β3* (*v*) transfected cells. The currents were evoked by depolarizing pulses to 10 mV from a holding potential of −60 mV (3000 ms in duration). Leak currents were subtracted using the P/4 protocol. *B*, effects of β subunits on the peak currents in CHO cells. *Each column and vertical bar* represents the mean ± S.E. The β subunits transfected into the cells are indicated at the *bottom*. The numbers of cells analyzed in this experiment are as follows: α_{1C} alone ($n = 8$), β2a ($n = 8$), β2/3 ($n = 8$), and β3 ($n = 8$). *, $p < 0.05$ *versus* α_{1C}. *C*, effects of different β subunits on the time constants of I_{Ba} decay in CHO cells. Data are expressed as means ± S.E. The numbers of cells used in this experiment are as follows: α_{1C} alone ($n = 8$), β2a ($n = 8$), β2/3 ($n = 8$), and β3 ($n = 8$). The β subunits transfected into the cells are indicated at the *bottom*. *, $p < 0.05$ *versus* α_{1C}.

effect on the current decay in the smooth muscle cells was due to the β3 gene manipulation, although isolated smooth muscle cells showed very accelerated current decays, which were probably due to other factors.

DISCUSSION

In the present study, we demonstrated a significant reduction in the L-type Ca^{2+} channel population in the aorta of $\beta3^{-/-}$ mice by Western blot and DHP binding analyses. We also found that the $\beta3^{-/-}$ phenotype resulted in reduced and slowly inactivated Ca^{2+} channel currents in aortic smooth muscle cells and decreased responsiveness to diltiazem in the global $[Ca^{2+}]_i$, whereas there were no changes in the Ca^{2+} sparks in mesenteric arteries.

In addition, disruption of the voltage-dependent calcium channel β3 subunit gene resulted in a decrease in responsiveness to DHP, as demonstrated by blood pressure measurement, and an increase in blood pressure in animals fed a high salt diet, as well as subsequent pathological changes such as hypertrophy of the aortic smooth muscle layer and cardiac enlargement.

We found a marked reduction in the channel population at the cell membrane in the aorta in $\beta3^{-/-}$ mice by biochemical methods, and our electrophysiological results, *i.e.* decreased peak currents and DHP sensitivity, strongly suggest a reduction in the DHP-sensitive calcium channel population. The results of several previous studies support the idea that the β subunits have a trafficking effect and increase the channel population (22, 23). In contrast, Neely *et al.* (24) reported that the β2 subunit does not influence gating currents, which is a charge movement of the voltage sensor, and should correspond to the channel population. Our results with $\beta3^{-/-}$ mice support the former idea, at least in the cardiovascular system.

In this study, we found a reduction of only 30% in the whole-cell Ca^{2+} channel currents in $\beta3^{-/-}$ cells, whereas overexpression experiments demonstrated a more marked effect of the β3 subunit, as compared with the results obtained with α_{1C} subunit-expressing cells (Fig. 5). As we found expression of the β2 subunit in the aorta, we further compared the effects of co-expression of the β2 and α_{1C} subunits with co-expression of both the β2 and β3 subunits and the α_{1C} subunit. The differences between these two conditions were apparently similar to those between $\beta3^{+/+}$ and $\beta3^{-/-}$ cells. The expression of the β2 subunit, as revealed in the RT-PCR experiment (Fig. 1*A*), suggests that the β2 subunit also interacts with α_{1C} subunits in the aortic smooth muscle cells *in vivo*. Of all known β subunits, recombinant rabbit β3 subunit has the strongest effect in accelerating the inactivation rate (9); the slow inactivation rate in $\beta3^{-/-}$ cells determined in the present study is also consistent with these observations. Therefore, our biochemical and electrophysiological results suggest that the heterogeneity of voltage-dependent calcium channels in vascular smooth muscle cells is at least partially due to the heterogeneous expression of the two β subunits, β2 and β3. It is likely that β2 is responsible for the relatively long-lasting L-type calcium channel currents in vascular smooth muscle cells. Furthermore, a recent study revealed an increase in a truncated form of the β3 subunit in human heart failure, suggesting the importance of the β3 subunit in cardiovascular function and the involvement of this subunit in pathological status (25).

We found no significant changes in local Ca^{2+} events, such as sparks and waves, in $\beta3^{-/-}$ mice, although significant differences in responsiveness to diltiazem were detected in global $[Ca^{2+}]_i$ elevation induced by 30 mM K^+ as compared with wild-type controls. Local intracellular calcium transients, Ca^{2+} sparks, are caused and regulated by the combined actions of VDCC, ryanodine-sensitive calcium release (RyR) channels, and Ca^{2+} pumps in the sarcoplasmic reticulum (26). The major physiological role of Ca^{2+} sparks in smooth muscle is the regulation of membrane potential via the activation of large conductance Ca^{2+}-sensitive K^+ (BK_{Ca}) channels, which represent a tripartite functional unit with VDCC and RyR (26, 27). A single Ca^{2+} spark is capable of producing a large local increase in $[Ca^{2+}]_i$ but has little effect on the global $[Ca^{2+}]_i$. As L-type calcium channel activation is known to increase the frequency and amplitude of Ca^{2+} sparks, our mouse model, in which the calcium channel current density is reduced by 30%, was used to examine Ca^{2+} sparks. Although we found no significant changes in Ca^{2+} sparks in $\beta3^{-/-}$ mice, L-type calcium channels play a significant role in the control of Ca^{2+} sparks, as diltiazem showed a significant inhibitory effect on their frequency and amplitude. This suggests that the enhanced Ca^{2+} influx through channels, including the β3 subunit during exposure to 30 mM K^+, neither contributes significantly to the amount of Ca^{2+} release per Ca^{2+} spark nor to the cycling rate of Ca^{2+} release from, and refilling of, the sarcoplasmic reticulum. The mutant mice used in the present study have a congenital 30% reduction in the calcium current density, and thus the regula-

tory mechanisms of $[Ca^{2+}]_i$ in smooth muscle cells could be modified in a compensatory manner during development. Changes in expression levels of related molecules, including RyR, BK channels, Ca^{2+} pump, and Na^+-Ca^{2+} exchanger, remain to be determined. Alternatively, the functional coupling of $\alpha_{1C}/\beta3$ channels with RyR may not be as tight as that of $\alpha_{1C}/\beta2$ channels, although this is unlikely, based on the uniform distribution of α_{1C} in $\beta3^{-/-}$ and $\beta3^{+/+}$ mice. In addition, the technical limits of laser-confocal microscopy, especially its temporal resolution, would make it difficult to detect slight differences in spark parameters due to the 30% reduction in peak calcium channel current.

We found no significant differences in blood pressure between $\beta3^{+/+}$ and $\beta3^{-/-}$ mice on the normal diet. As calcium channels are thought to play important roles in maintaining the cardiovascular tonus by regulating calcium influx into smooth muscle cells, there must be a compensatory mechanism for the decreased channel population in $\beta3^{-/-}$ mice. On the other hand, we detected decreased responsiveness to the DHP analogue amlodipine in the results of blood pressure measurement. As we found a significant reduction in the channel population, based on the results of biochemical analysis, and decreased DHP sensitivity in electrophysiological experiments, the decreased responsiveness to amlodipine in the blood pressure measurement clearly coincided with the decreased channel population and reduced electrophysiological DHP responsiveness in the patch clamp experiments, and was probably due to the same mechanism, *i.e.* the reduced channel population in the arterial smooth muscle cells.

The increase in blood pressure in response to salt loading is possibly related to sodium excretion and re-absorption in the kidney. Therefore, we examined calcium channel subunit gene expression in the kidney by *in situ* hybridization. We found no significant differences between $\beta3^{+/+}$ and $\beta3^{-/-}$ mice, except the lack of expression of the β3 calcium channel subunit in the mutants. There were also no morphological changes in the kidneys of $\beta3^{-/-}$ mice. Furthermore, we examined plasma renin concentrations, but no clear changes were detected because of the high degree of variance in the results. To date, no genes related to salt-sensitive hypertension have been mapped to human chromosome 12q13, the locus of the human homologue of β3 (10); however, as most such genes have yet to be isolated and are unmapped, this could be a candidate locus to examine for novel linkages in future studies. The pathological changes, *i.e.* cardiac enlargement and hypertrophic changes in the aortic smooth muscle layer, are common features in hypertensive animals and may be a consequence of the elevated blood pressure. As blood pressure is regulated through comprehensive integration of cardiac, neuronal, humoral, and vascular mechanisms, the loss of expression of a single voltage-dependent calcium channel β subunit is probably compensated for by some as yet unknown mechanism under basal conditions; however, this compensatory mechanism is not sufficient to maintain normal function under conditions of salt overload. Further studies are required to determine the mechanisms responsible for the observed salt sensitivity and the lack of changes in blood pressure in $\beta3^{-/-}$ mice.

Pharmacological modulation of the calcium channels is mainly due to their α_1 subunit, which is the target of many calcium channel blockers. The β subunit has been shown to affect the sensitivity of the channels to some calcium channel blockers (28, 29). Therefore, we examined the effects of both nicardipine and verapamil on contraction of the aortic smooth muscle cells, which might be affected by reduced L-type currents. However, we found no differences in the responses to these drugs between $\beta3^{+/+}$ and $\beta3^{-/-}$ mice (data not shown). As both the β2 and β3 genes are expressed in wild-type mice, the calcium channels are probably composed of a heterogeneous mixture of α_{1C}, β2, and β3 in aortic smooth muscle cells, and thus it might be difficult to detect significant differences merely by comparisons between $\beta3^{+/+}$ and $\beta3^{-/-}$ mice.

Taken together, the results of this study demonstrate that the β subunit determines the characteristics of calcium channels of vascular smooth muscle cells. We also demonstrated that the mouse voltage-dependent calcium channel β3 subunit gene product plays a role in the salt-sensitive blood pressure increase that is responsible for a number of pathological changes.

Acknowledgments—We thank Hirotaka Tanabe, Testuko Sueta, Alexandra Bhöme, and Barbara Wallenwein for their technical assistance. We also thank Drs. Veit Flockerzi, Kazuo Nunoki, and Kyoichi Ono for their help.

REFERENCES

1. Hofmann, F., Biel, M., and Flockerzi, F. (1994) *Annu. Rev. Neurosci.* **17,** 399–418
2. Catterall, W. A. (2000) *Annu. Rev. Cell. Dev. Biol.* **16,** 521–555
3. Perez-Reyes, E., Cribbs, L. L., Daud, A., Lacerda, A. E., Barclay, J., Williamson, M. P., Fox, M., Rees, M., and Lee, J.-H. (1998) *Nature* **391,** 896–900
4. Pragnell, M., De Waard, M., Mori, Y., Tanabe, T., Snutch, T. P., and Campbell, K. P. (1994) *Nature* **368,** 67–70
5. De Waard, M., Witcher, D. R., Pragnell, M., Liu, H., and Campbell, K. P. (1995) *J. Biol. Chem.* **270,** 12056–12064
6. Singer, D., Biel, M., Lotan, I., Flokerzi, V., Hofman, F., and Dascal, N. (1991) *Science* **253,** 1553–1557
7. Tareilus, E., Roux, M., Qin, N., Olcese, R., Zhou, J., Stefani, E., and Birnbaumer, L. (1997) *Proc. Natl. Acad. Sci. U. S. A.* **94,** 1703–1708
8. Varadi, G., Lory, P., Schultz, D., Varadi, M., and Schwartz, A. (1991) *Nature* **352,** 159–162
9. Hullin, R., Singer-Lahat, D., Freichel, M., Biel, M., Dascal, N., Hofmann, F., and Flockerzi, V. (1992) *EMBO J.* **11,** 885–890
10. Collin, T., Lory, P., Taviaux, S., Courtieu, C., Guilbault, P., Berta, P., and Nargeot, J. (1994) *Eur. J. Biochem.* **220,** 257–262
11. Murakami, M., Yamamura, H., Murakami, A., Okamura, T., Nunoki, K., Mistui-Saito, M., Muraki, K., Hano, K., Imaizumi, Y., Flockerzi, V., and Yanagisawa, T. (2002) *J. Cardiovasc. Pharmacol.* **36,** S69–S73
12. Murakami, M., Fleischmann, B., De Felipe, C., Freichel, M., Trost, C., Ludwig, A., Wissenbach, U., Schwegler, H., Hofmann, F., Hescheler, J., Flockerzi, V., and Cavalie, A. (2002) *J. Biol. Chem.* **277,** 40342–40351
13. Kang, M.-G., Chen, C. C., Felix, R., Letts, V. A., Frankel, W. N., Mori, Y., and Campbell, K. P. (2001) *J. Biol. Chem.* **276,** 32917–32924
14. Witcher, D. R., DeWaad, M., Sakamoto, J., Franzini-Armstrong, C., Pragnell, M., Kahl, S. D., and Campbell, K. P. (1993) *Science* **261,** 486–489
15. Striessnig J., Goll, A., Moosburger, K., and Glossmann, H. (1986) *FEBS Lett.* **197,** 204–210
16. Imaizumi, Y., Muraki, K., and Watanabe, M. (1990) *J. Physiol.* (*Lond.*) **427,** 301–324
17. Neher, E. (1992) *Methods Enzymol.* **207,** 123–131
18. Bosse, E., Bottlender, R., Kleppisch, T., Hescheler, J., Welling, A., Hofmann, F., and Flockerzi V. (1992) *EMBO J.* **11,** 2033–2038
19. John, S. W. M., Krege, J. H., Oliver, P. M., Hagaman, J. R., Hodgin, J. B., Pang, S. C., Flynn, T. G., Smithies, O. (1995) *Science* **267,** 679–681
20. Welling, A., Bosse, E., Cavalié, A., Bottlender, B., Ludwig, A., Nastainczyk, W., Flockerzi, V., and Hofmann, F. (1993) *J. Physiol.* (*Lond.*) **471,** 749–765
21. Aoyama, M., Murakami, M., Iwashita, T., Ito, Y., Yamaki, K., and Nakayama, S. (2003) *Biophys. J.* **84,** 709–724
22. Bichet, D., Cornet, V., Geib, S., Carlier, E., Volsen, S., Hoshi, T., Mori, Y., and De Waard, M. (2000) *Neuron* **25,** 177–190
23. Nishimura, S., Takeshima, H., Hofmann, F., Flockerzi, V., and Imoto, K. (1993) *FEBS Lett.* **324,** 283–286
24. Neely, A., Wei, X., Olcese, R., Birnbauer, L., and Stefani, E. (1993) *Science* **262,** 575–578
25. Hullin, R., Khan, I. F. Y., Wirtz, S., Mohacsi, P., Varadi, G., Schwartz, A., and Herzig, S. (2003) *J. Biol. Chem.* **278,** 21623–21630
26. Jaggar, J. H., Porter, V. A., Lederer, W. J., and Nelson, M. T. (2000) *Am. J. Physiol.* **278,** C235–C256
27. Ohi, Y., Yamamura, H., Nagano, N., Ohya, S., Muraki, K., Watanabe, M., and Imaizumi, Y. (2001) *J. Physiol.* (*Lond.*) **534,** 313–326
28. Welling, A., Lacinova, L., Donatin, K., Ludwig, A., Bosse, E., Flockerzi, V., and Hofmann, F. (1995) *Pfluegers Arch.* **429,** 400–411
29. Lacinova, L., Welling, A., Bosse, E., Ruth, P., Flockerzi, V., and Hofmann, F. (1995) *J. Pharmacol. Exp. Ther.* **274,** 54–63